

# Generation of Multi-Color Attosecond X-Ray Radiation Through Modulation Compression

Ji Qiang\*

Lawrence Berkeley National Laboratory, Berkeley, CA 94720, USA

Juhao Wu

SLAC National Accelerator Laboratory, Menlo Park, CA 94025, USA

(Dated: February 24, 2011)

In this paper, we propose a scheme to generate tunable multi-color attosecond coherent X-ray radiation for future light source applications. This scheme uses an energy chirped electron beam, a laser modulators, a laser chirper and two bunch compressors to generate a multi-spike prebunched kilo-Ampere current electron beam from a few tens Ampere electron beam out of a linac. Such an electron beam transports through a series of undulator radiators and bunch compressors to generate multi-color coherent X-ray radiation. As an illustration, we present an example to generate two attosecond pulses with 2.2 nm and 3 nm coherent X-ray radiation wavelength and more than 200 MW peak power using a 30 Ampere 200 nm laser seeded electron beam.

PACS numbers: 29.27.Bd; 52.35.Qz; 41.75.Ht

Attosecond coherent X-ray source provides an important tool to study ultra-fast dynamic process in biology, chemistry, physics, and material science. In recent years, there is growing interest in generating attosecond X-ray radiation pulse using Free Electron Lasers (FELs) [1–8]. Most of those schemes generates a single color attosecond pulse X-ray radiation except that in reference [8], where two attosecond X-ray radiation pulses with different radiation wavelength (colors) were produced based on a recently proposed echo scheme [9]. Meanwhile, multi-color attosecond X-ray radiation has important applications in time-resolved experiments such as multidimensional X-ray spectroscopy by either exciting or probing different types of atom in a system [10]. In reference [8], the second color attosecond pulse radiation was produced using a few-cycle laser modulator, a bunch compressor, and a short undulator radiator. In this paper, we propose a scheme to generate such tunable multi-color attosecond coherent X-ray radiation based on an improved modulation compression method [11]. This scheme avoids the usage of an extra laser modulator to produce an extra color attosecond X-radiation in the reference 8. It also uses a low current (on the order of ten Amperes) electron beam out of a linac instead of a kilo-Ampere electron

beam used in the reference 8.

A schematic plot of the scheme to generate multi-color attosecond X-ray radiation is given in Fig. 1. It consists of an energy chirped electron beam, a seeding laser modulator, a bunch compressor A, a laser chirper, a bunch compressor B1, an undulator radiator one, a bunch compressor B2, another undulator radiator two, and a number of repeating bunch compressors and radiators for multi-color X-ray radiation. Assume an initial beam longitudinal phase space distribution of the beam as:

$$f(z, \delta) = F(z, (\delta - hz)/\sigma) \quad (1)$$

where  $z$  is the relative longitudinal distance with respect to the reference particle,  $\delta = \Delta E/E$  is the relative energy deviation,  $h$  is the initial beam energy chirp, and  $\sigma$  is the initial uncorrelated energy spread. By properly choosing the momentum compaction factor of bunch compressor B such that

$$R_{56}^b = -R_{56}^a/M \quad (2)$$

the longitudinal phase space distribution after the bunch compressor B1 can be written as:

$$f(z, \delta) = F(Mz, [\delta - M\tilde{h}z - MA \sin(kMz)]/M\sigma) \quad (3)$$

where

$$M = 1 + h_b R_{56}^a \quad (4)$$

represents the total modulation compression factor,  $\tilde{h} = h_b/C + h$ ,  $C$  is the compression factor from the first bunch compressor A,  $h_b$  is the energy chirp introduced by the laser chirper,  $R_{56}^a$  is the momentum compaction factor of the first bunch compressor,  $A$  is the modulation amplitude of the seeding laser in the unit of the relative energy, and  $k$  is the wave number of the seeding laser. The above distribution function represents a compressed modulation in a chirped beam. In the above equations, we have



FIG. 1: A schematic plot of the lattice layout of the modulation compression scheme.

\*Electronic address: jqiang@lbl.gov

also assumed a longitudinally frozen electron beam and a linear laser chirper instead of the real sinusoidal function from the laser modulator.

The linear chirp in Eq. 4 from a sinusoidal laser chirper modulation can be approximated as  $h_b = A_b k_b$ , where  $A_b$  is the amplitude of the laser modulation,  $k_b$  is the wavenumber of the laser. The sinusoidal form of the energy modulation provides periodical energy chirping/unchirping across the beam. If the amplitude envelop of the sinusoidal energy modulation is controlled externally, the periodical local chirping of the beam can be controlled. From Eq. 4, the local modulation compression factor can be controlled across the beam. This results in a periodically separated locally modulated beam with different modulation wavelengths. For a Gaussian laser beam, the energy modulation caused by the laser chirper can be given as:

$$\delta = \delta + A_b \sin(k_b z) \exp\left(-\frac{1}{2} \frac{z^2}{\sigma_b^2}\right) \quad (5)$$

where  $\sigma_b$  is the rms laser pulse length. The local linear chirp resulted from such a laser chirper at different wavelength separation will be

$$h_b(i\lambda) = A_b k_b \exp\left(-\frac{1}{2} \frac{(i\lambda)^2}{\sigma_b^2}\right) \quad (6)$$

where  $i = 0, \pm 1, \pm 2, \dots$ . Using Eq. 4, the resultant modulation compression factor  $M$  becomes

$$M(i\lambda) = 1 + A_b k_b \exp\left(-\frac{1}{2} \frac{(i\lambda)^2}{\sigma_b^2}\right) R_{56}^a \quad (7)$$

From above equation, we see that on either side of the Gaussian laser pulse (i.e.  $i \geq 0$ , or  $i \leq 0$ ), the compressed modulation wavelength will decrease with the increase of the separation. To achieve the final modulation compression, the  $R_{56}^b$  of the bunch compressor Bs after the laser chirper needs to match the condition 2. For the first local chirp  $h_b(0)$ , this can be done by using the bunch compressor B1. After the beam passes through the first radiator to generate first color radiation, the second bunch compressor B2 can be used to produce locally prebunched beam corresponding to the local chirp  $h_b(\lambda)$ . Such a locally prebunched beam passing through the second radiator will generate another color X-ray. Following the same procedure, multi-color X-ray radiation can be generated by using multiple of bunch compressor and radiator pairs for different local chirp  $h_b$  and modulation compression factor.

As an illustration of above scheme, we will produce two-color attosecond coherent X-ray radiation using a similar example in reference [8]. A short uniform electron bunch (100  $\mu\text{m}$ ) with 10 pC charge, 2 GeV energy,  $-54.45 \text{ m}^{-1}$  energy-bunch length chirp, and an uncorrelated energy spread of  $1 \times 10^{-6}$  is assumed at the beginning of the seeding laser modulator. The initial normalized modulation amplitude  $A$  is  $1.2 \times 10^{-6}$ . Assuming 1

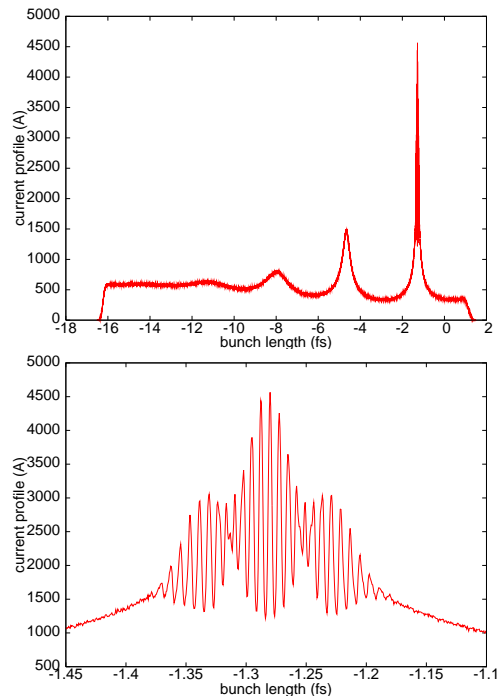


FIG. 2: Beam current distribution at the end of the bunch compressor B1 (top) and the zoom-in current distribution inside the first spike of the beam around  $z = 0$  (bottom).

Tesla magnetic field in the wiggler with a total length of 33 cm and a period of 11 cm, this corresponds to about 130 kW 200 nm wavelength laser power. After the modulator, we add an uncorrelated energy spread of 0.56 keV to the beam to account for the synchrotron radiation effects inside the wiggler magnet. After the initial seeding laser modulator, the beam passes through the chicane bunch compressor A. Here, we have assumed that the  $R_{56}$  of the chicane is 1.763 cm. This gives a factor of 25 compression from this bunch compressor. Another 0.63 keV uncorrelated energy spread is added to the beam to account for the uncorrelated energy spread growth from the quantum fluctuation of the incoherent synchrotron radiation through the chicane. After the beam passes through the chicane, it then transports through a short-pulse laser chirper with a 800 nm resonance wavelength. Here, we assumed that the energy modulation from the laser chirper follows a Gaussian envelop function as given in Eq. 5 with the rms laser pulse length  $\sigma_b = 1.307\lambda_b$ . The normalized amplitude of the laser for the first local chirp is chosen as  $6.29 \times 10^{-4}$  so that the total modulation compression factor is about 88.1. This modulation amplitude corresponds to about 38 GW laser power using a single wiggler period with 0.715 T magnetic field and 22.4 cm period length. After the beam transports through the laser chirper, it passes through a dog-leg type bunch compressor B1 that can provide opposite sign  $R_{56}^b$  compared to the chicane. For a total compression factor of 88.1 of the first local chirp, the  $R_{56}^b$  for the bunch compressor B1 is about  $-0.02 \text{ mm}$ . Fig. 2 shows the pro-

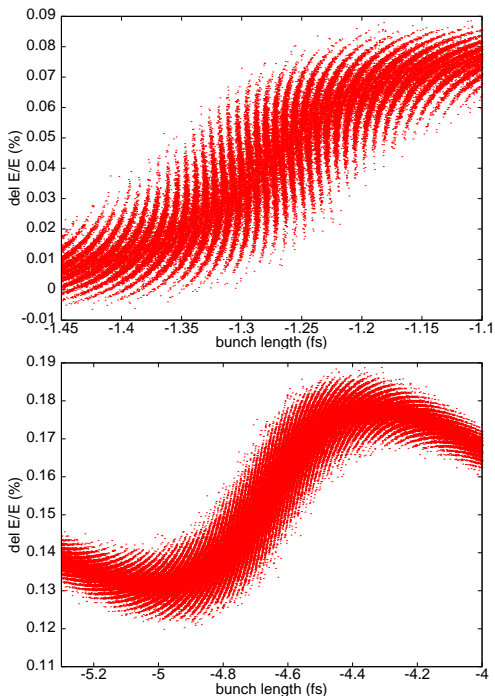


FIG. 3: Longitudinal phase space inside the first spike (top) and the second spike (bottom) of the beam at the end of the bunch compressor B1.

jected current profiles at the end of the bunch compressor B1. Here, only half of the laser pulse is used to unchirp the initial seeded beam in order to avoid the two locally prebunched attosecond beam with the same modulation wavelength due to the symmetry of the laser Gaussian envelope function. Given an initial 30 A beam current, the prebunched current inside the first spike with about 2.2 nm wavelength modulation reaches about 4.5 kA. The width of the prebunched beam is about two hundred attoseconds. This is set by the half wavelength of the laser chirper and the compression of the beam. There are other lower current spikes besides the first spike separated by laser chirper wavelength inside the beam. Those spikes will not contribute significantly to the 2.2 nm attosecond radiation since density microbunching in those spikes is very small due to the lower modulation compression factor and the mismatch of the  $R_{56}$  of the bunch compressor B1 at those spike locations. Fig. 3 shows the longitudinal phase space inside the first spike and the second spike of the beam. The particles inside the first spike of the beam are correctly modulated and compressed while the particles inside the second spike are over compressed and result in little current density modulation.

The above highly prebunched beam passing through a short undulator R1 will generate coherent attosecond X-ray radiation. Here, we have used the GENESIS simulation code [12] to calculate the coherent X-ray radiation through the short undulator radiator. The normalized emittance of the electron beam is chosen to be  $0.2 \mu\text{m}$ . The length of the radiator is about 1.0 m with an un-

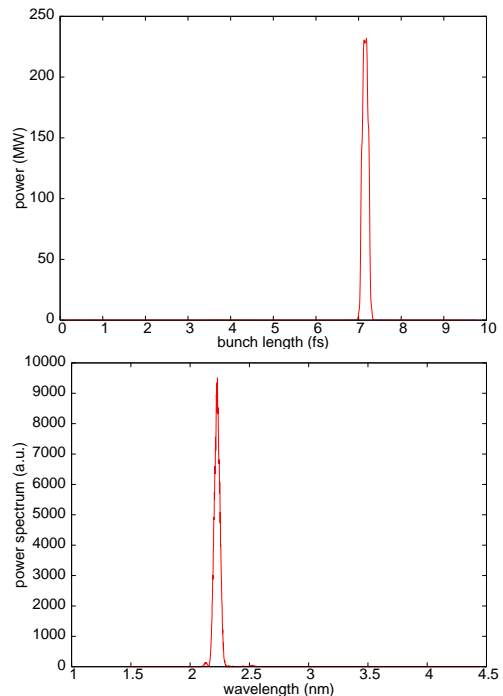


FIG. 4: The radiation pulse temporal profile (top) and the radiation pulse spectral profile (bottom) at the end of the undulator radiator 1.

dulator period of 3.33 cm. The details of the radiation properties at the end of the radiator R1 are shown in Fig. 4. The full width at half maximum of the radiation pulse is about 200 as. The peak radiation power is beyond 220 MW.

After the electron beam passes through the radiator R1, the output longitudinal particle distribution from the previous GENESIS simulation is used to pass through the bunch compressor B2. The  $R_{56}$  of this bunch compressor is chosen to be about  $-61.7 \mu\text{m}$  so that the modulation compression condition 2 can be satisfied for the second current spike inside the beam. This results in a modulation compression factor of about 66.0 inside that local spike. Fig. 5 shows the longitudinal phase space and current profile inside the second current spike of the beam at the end of the bunch compressor B2. It is seen that after this bunch compressor, the beam is significantly modulated with a wavelength about 3 nm inside the second spike. The peak current inside this spike is about 2.6 kA with a modulation width of about 200 as. The energy spread inside this spike is still small and there is a total upshift of the energy due to the global energy chirp of the beam. Such an upshift could also help separate the radiation of this local current spike from that of the other local current spikes inside the undulator. Fig. 6 shows the radiation pulse power temporal profile and the radiation pulse spectral profile at the end of the radiator R2. Here, we have assumed that the radiator is 4.45 m long with an undulator period of 4.45 cm. The full width at half maximum of the radiation pulse is about

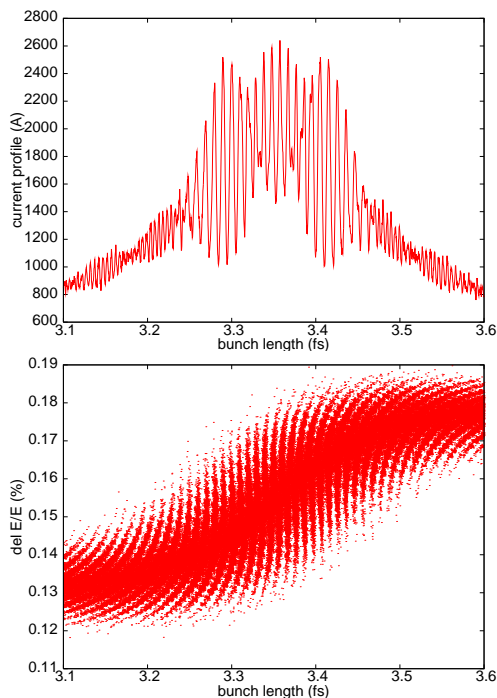


FIG. 5: Longitudinal phase space (top) and current profile (bottom) of the second spike at the end of the bunch compressor B2.

400 as with a radiation peak power more than 210 MW. The radiation pulse length is longer than the width of

the modulated current density distribution. This is due to the slippage of the photon pulse with respect to the electron bunch inside the radiator.

In this paper, we proposed a scheme to generate multi-color attosecond coherent X-ray radiation through modulation compression by using a low current chirped electron beam. This scheme allows one to tune the final X-ray radiation wavelength by adjusting the compression factor. It also allows one to control the final radiation pulse length by controlling the laser chirper parameters and the initial compression parameters. Some technical challenges such as keeping good synchronization between the electron beam and the laser beam and controlling the laser power jitter can be solved with the fast advances of the instrumentation and the laser technology.

### Acknowledgments

We would like to thank Dr. J. Corlett for useful discussions and Dr. M. Reinsch for the discussion about the GENESIS usage. This research used computer resources at the National Energy Research Scientific Computing Center. The work of JQ was supported by the U.S. Department of Energy under Contract No. DE-AC02-05CH11231 and the work of JW was supported by the U.S. Department of Energy under contract DE-AC02-76SF00515.

- 
- [1] A.A. Zholents and W.M. Fawley, Phys. Rev. Lett. **92**, 224801 (2004).
  - [2] A.A. Zholents and G. Penn, Phys. Rev. ST Accel. Beams **8**, 050704 (2005)
  - [3] E.L. Saldin, E.A. Schneidmiller, and M.V. Yurkov, Phys. Rev. ST Accel. Beams **9**, 050702 (2006)
  - [4] J. Wu, P.R. Bolton, J.B. Murphy, K. Wang, Optics Express **15**, 12749, (2007).
  - [5] A.A. Zholents and M.S. Zolotarev, New Journal of Physics **10**, 025005 (2008).
  - [6] Y. Ding, et al., Phys. Rev. ST Accel. Beams **12**, 060703 (2009).
  - [7] D. Xiang, Z. Huang, and G. Stupakov, Phys. Rev. ST Accel. Beams **12**, 060701 (2009).
  - [8] A.A. Zholents and G. Penn, Nucl. Instr. Meth. A **612**, 254 (2010).
  - [9] G. Stupakov, Phys. Rev. Lett **102**, 074801 (2009).
  - [10] S. Tanaka, and S. Mukamel, Phys. Rev. Lett., **89**, 043001 (2002).
  - [11] J. Qiang and J. Wu, "Generation of coherent X-ray radiation through modulation compression," arXiv: physics.acc-ph/1012.5446v1, 2010.
  - [12] S. Reiche, Nucl. Instr. and Meth. A **429**, 243 (1999).

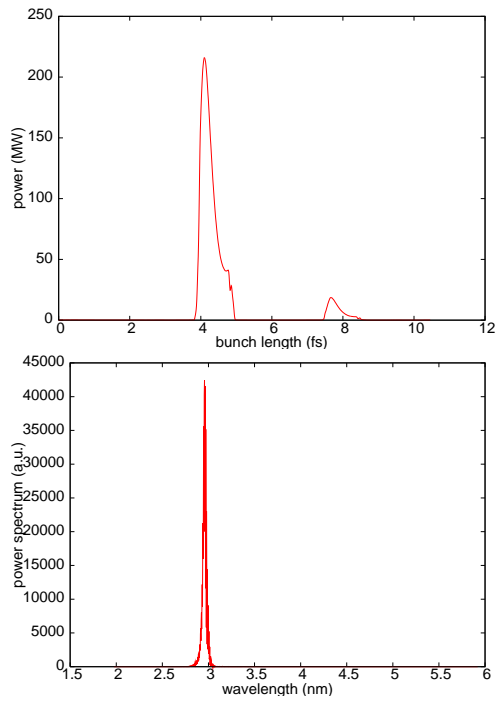


FIG. 6: The radiation pulse temporal profile (top) and the radiation pulse spectral profile (bottom) at the end of the undulator radiator 2.